A Pared-Down Version of 5,10,15,20-Tetra(*N*-methylpyridinium-4-yl)porphyrin Intercalates into B-Form DNA Regardless of Base Composition: Binding Studies of Tri(*N*-methylpyridinium-4-yl)porphyrins†

Kim Andrews and David R. McMillin*

Department of Chemistry, 560 Oval Drive, Purdue University, West Lafayette, Indiana 47907-2084

Received September 13, 2007; Revised Manuscript Received November 13, 2007

ABSTRACT: Positively charged *N*-methylpyridinium-4-yl substituents promote the binding of a porphyrin to DNA, but they also impose steric constraints. To clarify when intercalative binding is most feasible, this report describes syntheses and binding studies of two tricationic ligands: 5,10,15-tri(*N*-methylpyridinium-4-yl)porphyrin (H_2Tri4) and 5-methyl-10,15,20-tri(*N*-methylpyridinium-4-yl)porphyrin (H_2MeTri4). Techniques used to characterize the binding interactions include viscometry and spectroscopic studies of the absorption, emission, and circular dichroism. The striking observation is that intercalation is the only detectable binding motif when the trisubstituted porphyrin H_2Tri4 combines with $[poly(dA\text{-}dT)]_2$, $[poly(dG\text{-}dC)]_2$, or salmon testes DNA. H_2Tri4 is, however, a limiting case. Parallel studies of H_2MeTri4 and the copper(II) derivative Cu(MeTri4) reveal that external binding to $[poly(dA\text{-}dT)]_2$ becomes important when a fourth meso substituent is present, even one as small as the methyl group. Intercalation of H_2Tri4 is sterically feasible because two *N*-methylpyridinium-4-yl substituents can reside in the major groove, though the charge alignment is not optimal. However, the presence of the fourth substituent on H_2MeTri4 further destabilizes the intercalated form, and external binding becomes competitive for a flexible host like $[poly(dA\text{-}dT)]_2$.

This investigation focuses on the impact that accumulating steric bulk has on the uptake of a tricationic porphyrin by B-form DNA. Structure−function correlations involving porphyrins are important in many applications including therapeutics. In the specific area of photodynamic therapy (PDT[1]), porphyrins function as effective sensitizers because of the long-wavelength visible absorption (*1*, *2*). Cationic forms hold promise for PDT applied to managing the treatment of antibiotic-resistant bacteria (*3*). In a broader context, cationic porphyrins like 5,10,15,20-tetra(*N*-methylpyridinium-4-yl)porphyrin (H_2T4 in Scheme 1) have historically received attention because they are water-soluble and naturally drawn to the DNA polyanion. Published evidence that H_2T4 is capable of penetrating cells and interacting with nuclei justifies continuing interest (*4*). Another observation fueling efforts is that H_2T4 has proven to be an inhibitor of telomerase, a DNA-extending enzyme that affects the longevity of tumor cells (*5*). One reason may be that H_2T4 is an avid ligand for DNA quadruplexes (*6*−*8*). H_2T4 and derivatives thereof are no less interesting as versatile ligands for double-stranded DNA (*9*, *10*). Despite many studies, however, questions about DNA-binding interactions remain unanswered. External, or groove, binding is the usual motif for metalated derivatives that retain one or more axial ligands (*11*−*13*). However, for H_2T4 itself or a metalated form lacking axial ligands, the nature of the complex varies with the base composition the DNA host.

† The National Science Foundation supported this work through Grant CHE-0550241. K.A. also acknowledges receipt of past support from NSF Grant IGERT-9987576, administered by the Krannert School at Purdue.

* Corresponding author: phone 765-494-5452; fax 765-494-0239; e-mail mcmillin@purdue.edu.

[1] Abbreviations: H_2T4, 5,10,15,20-tetra(*N*-methylpyridinium-4-yl)-porphyrin; H_2Tri4, 5,10,15-tri(*N*-methylpyridinium-4-yl)porphyrin; H_2-MeTri4, 5-methyl-10,15,20-tri(*N*-methylpyridinium-4-yl)porphyrin; $[poly(dA\text{-}dT)]_2$, sodium salt of poly(deoxyadenylic-deoxythymidylic) acid; $[poly(dG\text{-}dC)]_2$, sodium salt of poly(deoxyguanylic-deoxycytidylic) acid; ST DNA, salmon testes deoxyribonucleic acid; Cu(MeTri4), (5,-10,15-tri(*N*-methylpyridinium-4-yl)porphyrinato)copper(II); PDT, photodynamic therapy; A or a, adenine; T or t, thymine; C or c, cytosine; G or g, guanine; A═T, adenine−thymine base pair; G≡C, guanine−cytosine base pair; Cu(T4), (5,10,15,20-tetra(*N*-methylpyridinium-4-yl)porphyrinato)copper(II); ^{1}H NMR, proton nuclear magnetic resonance; H_2D3, 5,15-di(*N*-methylpyridinium-3-yl)porphyrin; H_2D4, 5,15-di(*N*-methylpyridinium-4-yl)porphyrin; H_2tMe_2D4, 5,15-dimethyl-10-20-di(*N*-methylpyridinium-4-yl)porphyrin; DMF, *N*,*N*-dimethylformamide; DMSO, dimethyl sulfoxide; {TT(ga_3)}, 5′-GATTACgaaaGTAATC-3′; {TT(t_4)}, 5′-GATTACttttGTAATC-3′; {CA(t_4)}, 5′-GACAACttttGT-TGTC-3′; {CA(ga_3)}, 5′-GACAACgaaaGTTGTC-3′; H_2Tri4*n*, 5,10,-15-tri(pyrid-4-yl)porphyrin; H_2MeTri4*n*, 5-methyl-10,15,20-tri(pyrid-4-yl)porphyrin; 5-Py-DPM, 5-(4-pyridyl)dipyrromethane; 5-Me-DPM, 5-methyldipyrromethane; DPM, dipyrromethane; MALDI-MS, matrix-assisted laser desorption ionization mass spectrometry; ppm, parts per million; ϵ, molar extinction coefficient; ψ', ellipticity; *l*, path length; % H, percent hyperchromism; μ, ionic strength; η, specific viscosity; SRV, standard reduced viscosity ratio; η/η_0, standard reduced viscosity; t_0, flow time of the buffer; t_D, flow time of the DNA in buffer; t_c, flow time with porphyrin and DNA; EI-MS, electron ionization mass spectrometry; CD, circular dichroism; *q*, base-pair-to-porphyrin ratio; Cu(tMe_2D4), (5,15-dimethyl-10,20-di(*N*-methylpyridinium-4-yl)porphyrinato)copper(II); ZnT4, (5,10,15,20-tetra(*N*-methylpyridinium-4-yl)porphyrinato)zinc(II); Zn(tMe_2D4), (5,15-dimethyl-10,20-di(*N*-methylpyridinium-4-yl)porphyrinato)zinc(II); Zn(D4), (5,15-di(*N*-methylpyridinium-4-yl)porphyrinato)zinc(II); NiT4, (5,10,15,20-tetra(*N*-methylpyridinium-4-yl)porphyrinato)nickel(II).

10.1021/bi7018755 CCC: $40.75
Published on Web 01/03/2008

Scheme 1

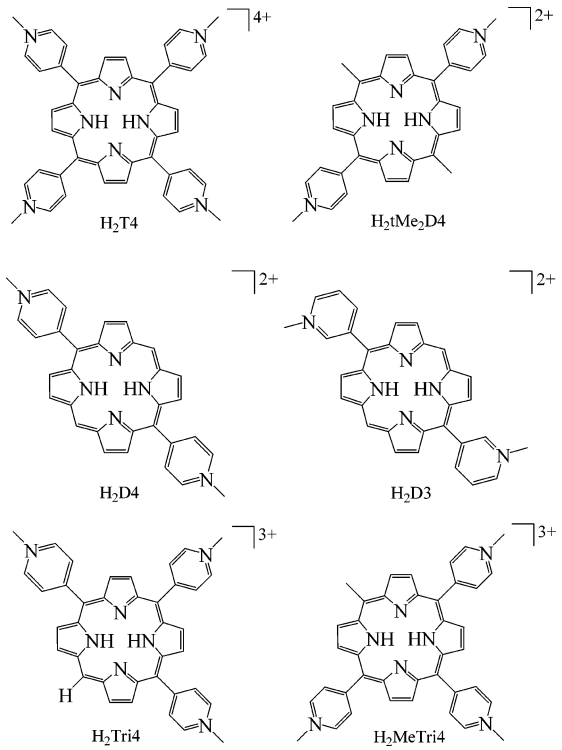

More specifically, external binding tends to occur in DNA sequences that are rich in adenine−thymine (A=T) base pairs while intercalation is the preferred binding motif in G≡C (guanine−cytosine) rich sequences (*9*−*11*). Although the hydrophobic effect undoubtedly has a role, charge and size considerations are major factors that shape the binding to DNA (*14*−*16*). Early systematic studies by Sari et al. (*17*) established that the electrostatic charge has a demonstrable influence on binding within a series of porphyrins exhibiting similar steric requirements. Much later, Williams and co-workers (*18*) published a crystal structure that exposed perhaps the most important steric problem associated with intercalative binding. Their structure dealt with a 6-mer duplex interacting with Cu(T4), the copper(II)-containing derivative of H_2T4. The results suggested that the two *N*-methylpyridinium-4-yl groups of the porphyrin that reside in the minor groove clash against the sugar−phosphate chains of the host. It is possible that solid-state forces influence the structure, however, because a subsequent ^{1}H NMR structure of an H_2T4 complex in solution did not report the same type of strain (*19*). Tensions between phases notwithstanding, McMillin and co-workers (*14*, *16*, *20*) have demonstrated that the sterically less demanding porphryins H_2D3 = 5,15-di(*N*-methylpyridinium-3-yl)porphyrin, H_2D4 = 5,15-di(*N*-methylpyridinium-4-yl)porphyrin, and H_2tMe_2-D4 = 5,15-dimethyl-10,20-di(*N*-methylpyridinium-4-yl)porphyrin (Scheme 1) all bind to B-form DNA exclusively by intercalation, independent of base composition. The results are consistent with the steric analysis of Williams and co-workers because the hallmark of all three ligands is that only one bulky pyridiniumyl group must enter into the minor groove.

If steric forces indeed destabilize the intercalated form, one may ask why H_2T4 intercalates into G≡C rich hosts. McMillin and co-workers (*15*, *16*, *21*) have inferred that a relatively rigid G≡C rich domain is resistant to the reorganization and/or melting of canonical DNA structure that *high-affinity* external binding evidently requires. An alternative explanation is that the porphyrin preferentially binds externally to an A=T-rich domain because the natural groove structure and/or associated electrostatic potential is extremely favorable (*22*, *23*). In fact, a published ^{1}H NMR structure assumes that external binding entails little structural change (*24*). The resolution of the problem clearly depends upon expanding the available database. This investigation focuses on the synthesis and investigation of the triply charged cationic porphyrins H_2Tri4 = 5,10,15-tri(*N*-methylpyridinium-4-yl)porphyrin and $H_2MeTri4$ = 5-methyl-10,15,20-tri(*N*-methylpyridinium-4-yl)porphyrin also illustrated in Scheme 1. The two systems offer an interesting new comparison because they bring to bear a common charge but different steric requirements.

EXPERIMENTAL PROCEDURES

Materials. Fisher Scientific or Mallinckrodt was the vendor for glacial acetic acid, $NaH_2PO_4 \cdot H_2O$, Na_2HPO_4, NaCl, NaOH, diethyl ether, methanol, dichloromethane, ethyl acetate, *n*-propyl alcohol, acetonitrile, hexane, hydrochloric acid, silica gel, sodium carbonate, sodium sulfate, zinc acetate, sulfuric acid, nitric acid, *N*,*N*-dimethylformamide (DMF), potassium carbonate, potassium nitrate, acetic anhydride, acetone, ammonium hydroxide, and chloroform. The alumina (80−200 mesh) came from EM Science, and the 8% cross-linked Dowex-1 strongly basic anion-exchange resin, chloride form (dry mesh 100−200), was from Acros. Sigma−Aldrich or Cambridge Isotope Laboratories was the supplier for deuterated chloroform ($CDCl_3$) and dimethylsulfoxide (DMSO). Sigma−Aldrich also sold the paraformaldehyde, 4-pyridinecarbaldehyde, acetaldehyde, copper acetate, dichlorodimethylsilane, Florisil (100−200 mesh), methyl-*p*-toluenesulfonate, potassium hexafluorophosphate (98%), sodium borohydride, tetrabutylammonium nitrate, Trizma base, Trizma hydrochloride, salmon testes (ST) DNA, and 2,6-lutidine as well as aluminum-backed silica gel thin-layer chromatography plates complete with fluorescent indicator. Pyrrole came from Sigma−Aldrich, Lancaster, or Acros Organics. GE Healthcare was the source of sonicated ST DNA and the sodium salt of poly(deoxyguanylic-deoxycytidylic) acid, or $[poly(dG\text{-}dC)]_2$ for short. The sodium salt of poly(deoxyadenylic-thymidylic) acid, or $[poly(dA\text{-}dT)]_2$, came from Midland Certified Reagent Co., Inc. Integrated DNA Technologies provided the 16-mer DNA hairpins listed in Scheme 2 with the shorthand names $\{TT(t_4)\}$, $\{TT(ga_3)\}$, $\{CA(t_4)\}$, and $\{CA(ga_3)\}$. The shorthand convention is that capital letters designate key bases of the stem domain, while lowercase letters code for the loop domain. The 0.22 and 0.45 μm filters came from Millipore Corp. Most commercial chemicals saw no purification, except the quality of the pyrrole improved after passage through a short alumina column. Deionized water also passed through a Barnstead Bantam purification system with a mixed-bed cartridge.

Syntheses. A MacDonald [2 + 2] type of procedure (*25*, *26*) yielded the neutral precursors H_2Tri4n = 5,10,15-tri(pyrid-4-yl)porphyrin and $H_2MeTri4n$ = 5-methyl-10,15,-20-tri(pyrid-4-yl)porphyrin. The method entails heating a stoichiometric amount of pyridine-4-carbaldehyde with an equimolar mixture of 5-Py-DPM = 5-(4-pyridyl)dipyr-

Scheme 2

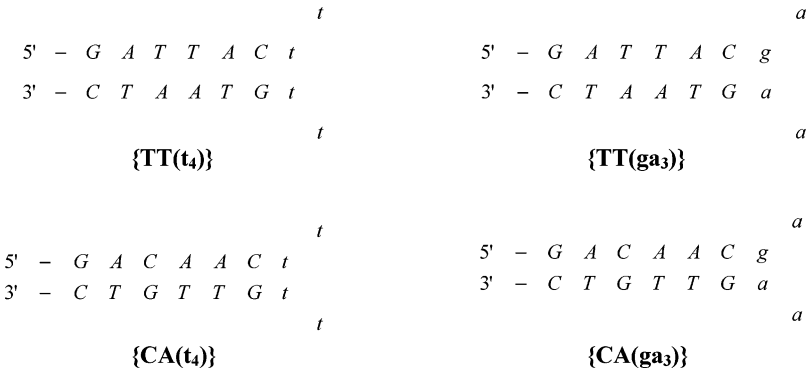

romethane (*27*) and either 5-Me-DPM = 5-methyldipyrromethane or DPM = dipyrromethane (*14*) in an acetic acid medium. Ambient dioxygen serves as the oxidizing agent. Three porphyrins form, but the desired tripyridylporphyrin is the statistically favored product in each instance. Anion exchange was possible by either of two methods. For example, the chloride salt deposited upon addition of a solution of tetrabutylammonium chloride in acetone to the hexafluorophosphate salt of the porphyrin dissolved in acetone. The other method involves stirring the porphyrin salt in methanol containing the chloride form of Dowex-1 resin and then filtering out the resin.

(A) H_2Tri4n. A combination of 2.0 mol equiv of 4-pyridinecarbaldehyde with 1.5 mol equiv of DPM and 0.5 mol equiv of 5-Py-DPM seemed to give the best yield of tripyridylporphyrin under the reaction conditions (*14*). After a batch extraction, elution with 20% acetone in dichloromethane removed the dipyridylporphyrin. The desired tripyridylporphyrin came off in combination with the tetrapyridylporphyrin with 2% methanol in dichloromethane. Subsequent chromatographic elutions with the same solvent systems ultimately afforded a separation of the tripyridyl- and tetrapyridylporphyrins. The solvent system used for recrystallization of H_2Tri4 contained methanol and diethyl ether. MALDI MS, m/z = 541; visible absorbance, λ_{max} (nm) = 411, 472, 502, 549, 645.

(B) H_2MeTri4n. The procedure is analogous to that described above and involved combining 2 mol equiv of 4-pyridinecarbaldehyde with 1.25 mol equiv of 5-Me−DPM and 0.75 mol equiv of 5-Py-DPM. MALDI MS, m/z = 555; visible absorbance, λ_{max} (nm) = 416.5, 513.5, 547, 588, 646.

(C) 5-Methyl-10,15,20-tri(N-methylpyridinium-4-yl)porphyrin Hexafluorophosphate Salt. The methylation reaction occurred in DMF upon heating a mixture of 0.054 mmol of H_2MeTri4*n*, 23.4 mmol of potassium carbonate, and 16.3 mmol of methyl-*p*-toluenesulfonate. After the reaction, the porphyrin precipitated upon addition of tetrabutylammonium nitrate in acetone. Dissolution of the nitrate salt into dilute aqueous HCl gave a green solution. After being stirred overnight, the solution yielded the red-brown hexafluorophosphate salt upon addition of aqueous KPF_6. The recrystallization medium was a 1:3 mixture of methanol and propanol. The final treatment involved heating the solid under vacuum in a drying pistol. ^{1}H NMR in DMSO-d_6: δ = 10.11 (d, 2H), 9.5−9.6 (overlapped, 6H), 9.1−9.2 (overlapped, 6H), 9.04 (d, 4H), 9.02 (d, 2H), 4.84 (s, 3H), 4.79 (s, 6H), 4.76 (s, 3H). H_2MeTri4·$(PF_6)_3$·0.5H_2O: Calcd for $C_{39}H_{33}N_7P_3F_{18}$·0.5H_2O 44.84 C, 3.37 H, 9.38 N; found 44.56 C, 3.46 H, 9.21 N. MALDI MS m/z = 600.2.

(D) 5,10,15-Tri(N-methylpyridinium-4-yl)porphyrin Hexafluorophosphate Salt. A similar procedure produced H_2Tri4 which eluted as a single peak on a thin-layer plate developed with the solvent system of Batinic-Haberle et al. (*28*). A metathesis procedure gave the hexafluorophosphate salt of the H_2Tri4 cation. ^{1}H NMR in DMSO-d_6: δ = 10.83 (s, 1H), 9.86 (d, 2H), 9.34−9.42 (overlapped, 6H), 9.25 (d, 2H), 9.19 (AB quartet, 4H), 8.99 (d, 4H), 8.94 (d, 2H), 4.76 (br s, 9H). In principle, the pyrrolic hydrogens exhibit four distinct chemical shifts. Due to the ring current effects of the neighboring out-of-plane pyridines (*29*), three of the four appear in the range of 9.1−9.3 ppm, upfield from the C2 and C18 hydrogens, which resonate as a doublet at 8.99 ppm. The counterpart doublet from the C3 and C17 hydrogens centers around 9.25 ppm. Here the other pyrrolic hydrogens resonate as an AB quartet, whereas a previous study employed a higher-field magnet and recorded a doublet of doublets (*7*). MALDI MS m/z = 586.2.

(E) Cu(MeTri4). The copper(II) derivative of H_2MeTri4 formed upon exposure of a solution of the porphyrin to 2 mol eqiov of copper(II) acetate in deionized water at 60 °C under a nitrogen atmosphere. As the product formed, the original four Q-bands in the absorption spectrum coalesced into two, and the fluorescence signal from H_2MeTri4 all but disappeared.

(F) Methods for Physical Studies. A siliconization procedure minimized adhesion of porphyrins to glassware used in spectral studies (*30*). Equation 1 provided a means for converting circular dichroism data from millidegrees to M^{-1} cm^{-1} units:

$$\epsilon = \psi'/(32\,980lc) \quad (1)$$

where ψ' is the original data in millidegrees, l is the path length, and c is the molar concentration. The percent decrease in the absorption intensity came from the following equation:

$$\%\,H = 100 - [(A_{DNA}/A)100] \quad (2)$$

where % H is the percent hyperchromism, A_{DNA} is the absorbance at the Soret maximum of the DNA complex, and A is the corresponding absorbance in the absence of DNA.

The calculation of concentrations involved the use of absorbance measurements in conjunction with Beer's law. Beer's law plots yielded ϵ_{417} = 198 000 M^{-1} cm^{-1} for H_2Tri4 and $\epsilon_{421.5}$ = 200 000 M^{-1} cm^{-1} for H_2MeTri4 in μ =

0.05 M Tris buffer, pH 7.5. The estimate for the molar extinction for Cu(MeTri4) came from the average of those reported for Cu(tMe$_2$D4) and Cu(T4) which are $\epsilon_{418.5}$ = 170 000 M^{-1} cm^{-1} and $\epsilon_{423.5}$ = 231 000 M^{-1} cm^{-1}, respectively (*16*, *31*). The porphyrin concentration was typically 1.7 μM for spectrophotometric investigations. The molar extinction coefficients used for DNA samples included ϵ_{260} = 13 600 M^{-1} cm^{-1} for [poly(dA-dT)]$_2$ (*32*), ϵ_{254} = 16 800 M^{-1} cm^{-1} for [poly(dG-dC)]$_2$ (*33*), ϵ_{260} = 13 200 M^{-1} cm^{-1} for ST DNA (*34*), all in units of base pairs. Literature values were available for some of the DNA hairpins, namely ϵ_{260} = 142 000 M^{-1} cm^{-1} for {TT(t$_4$)}, ϵ_{260} = 166 000 M^{-1} cm^{-1} for {TT(ga$_3$)}, and ϵ_{260} = 109 000 M^{-1} cm^{-1} for {CA(t$_4$)} (*35*). The near-neighbor method yielded an estimated value of ϵ_{260} = 162 000 M^{-1} cm^{-1} for {CA(ga$_3$)} (*36*).

For viscometry studies, the solution contained ST DNA at a concentration of 70 μM in base pairs. After sonication, the average length of the DNA molecules was about 300 base pairs as established by gel electrophoresis. Equation 3 gave the calculated standard reduced viscosity (SRV) ratio:

$$\frac{\eta}{\eta_0} = \frac{t_c - t_0}{t_D - t_0} \quad (3)$$

where t_0 was the flow time of the buffer, t_D was the flow time of DNA in buffer, and t_c was the flow time of the DNA solution containing porphyrin (*37*). For each measurement at 28 °C, the experimental flow time was an average of the first three consecutive runs that agreed with each other to within ±1 s.

Instrumentation. Absorbance data came from a Varian Cary 100 Bio UV-spectrophotometer, while the luminescence instrument was a Varian Cary Eclipse fluorescence spectrophotometer. The CD instrument was a Jasco J810 spectropolarimeter. The microwave oven was a commercial Kenmore household microwave model. ^{1}H NMR data came from 200 or 300 MHz Varian Mercury Inova spectrometers. The Purdue University Campus-wide Mass Spectrometry Center performed the MALDI and EI mass spectral measurements.

RESULTS

Data reported in Table 1 illustrate how the spectroscopic properties of the complexes vary with the composition of the DNA host. Thus, when [poly(dA-dT)]$_2$ is the host, interaction with H$_2$T4 induces a weak hypochromic response in the absorption spectrum and a positive CD signal (Figure 1). In contrast, there is a strong hypochromic response and a negative CD signal when [poly(dG-dC)]$_2$ acts as the host (Table 1). When the host is random sequence DNA from ST DNA, the results are more or less the arithmetic sum of the above. Thus, the hypochromic response falls in between the values obtained with [poly(dA-dT)]$_2$ and [poly(dG-dC)]$_2$, and the CD signal has a positive as well as a negative maximum, with the positive band at shorter wavelengths. The less bulky trisubstituted porphyrin H$_2$Tri4, on the other hand, apparently adopts only one mode of binding. Regardless of the host, interaction with DNA induces a marked hypochromic response and a negative CD signal in the Soret region. Figure 1 includes the CD spectrum of the complex formed with [poly(dA-dT)]$_2$.

The H$_2$MeTri4 system therefore proves to be a critical member of the series. It carries four substituents in the meso positions, but one is a comparatively small methyl group. When [poly(dG-dC)]$_2$ interacts with H$_2$MeTri4, the spectral changes parallel those observed with H$_2$Tri4 and H$_2$T4. However, interaction of H$_2$MeTri4 with [poly(dA-dT)]$_2$ induces a bisignate CD signal (Figure 1), along with a Soret shift and hypochromic response of intermediate magnitude. All three observations are consistent with the simultaneous formation of two types of complexes with [poly(dA-dT)]$_2$. The fact that H$_2$MeTri4 exhibits the same CD signal at μ = 0.05 and μ = 0.15 M in the presence of excess [poly(dA-dT)]$_2$ argues against an interpretation based on exciton

Table 1: Spectral Data for Porphyrins Interacting with DNA in μ = 0.05 M Tris Buffer, pH 7.5

		Soret absorption		CD	
porphyrin	DNA[a]	$\Delta\lambda$,[b] nm	% H[c]	λ, nm	$\Delta\epsilon$, M^{-1} cm^{-1}
H$_2$T4[d]	[poly(dA-dT)]$_2$	9	3	430	+28
H$_2$T4[d]	[poly(dG-dC)]$_2$	23	46	443	−12
H$_2$T4[d]	ST DNA	10	36	427, 449	+10, −8
H$_2$Tri4	[poly(dA-dT)]$_2$[d]	18	32	440	−18
H$_2$Tri4	[poly(dG-dC)]$_2$	26	44	442	−14
H$_2$Tri4	ST DNA	21	28	439	−17
H$_2$MeTri4	[poly(dA-dT)]$_2$[d]	13	17	428, 449	+20, −7
H$_2$MeTri4	[poly(dG-dC)]$_2$	28	44	449	−25
H$_2$MeTri4	ST DNA	23	34	447	−15
H$_2$MeTri4	{CA(t$_4$)}[e]	18	23	422, 447	+4, −11
H$_2$MeTri4	{CA(ga$_3$)}[f]	21	22	446	−22
Cu(MeTri4)	[poly(dA-dT)]$_2$	8	−13	420, 439	+45, −35

[a] DNA base pair to porphyrin ratio ≥40:1 except as noted to ensure saturation. [b] Bathochromic shift of Soret maximum. [c] Hypochromism defined as the percent drop in intensity of the absorbance maximum. [d] Data from a μ = 0.15 M buffer, pH 7.5. [e] 16-mer to porphyrin ratio of 4.2:1. [f] 16-mer to porphyrin ratio of 8.5:1.

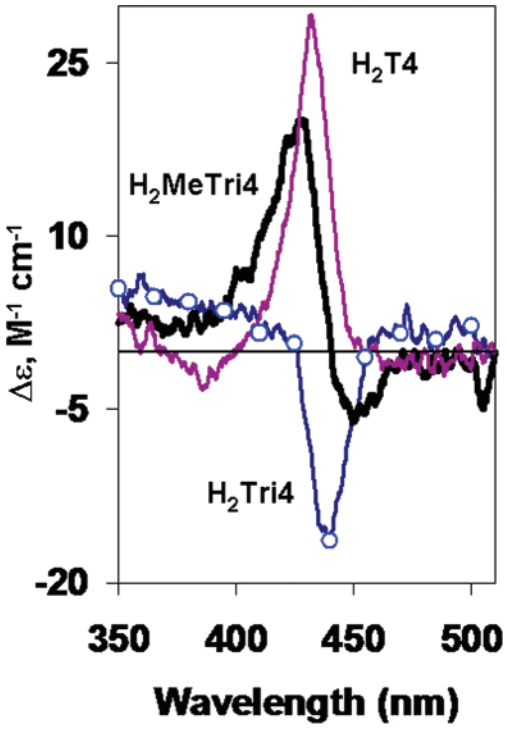

FIGURE 1: CD spectra in μ = 0.15 M Tris buffer, pH 7.5, with 50 base pairs of [poly(dA-dT)]$_2$ per unit of porphyrin. The porphyrins are H$_2$T4 (thin purple trace), H$_2$Tri4 (thin blue trace with circles), and H$_2$MeTri4 (thick black trace).

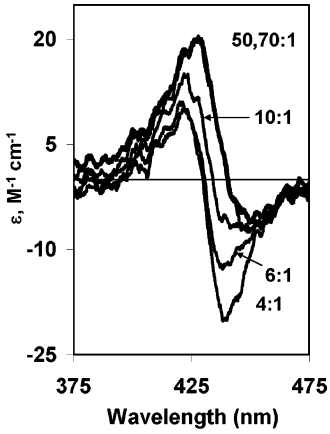

FIGURE 2: CD spectra in $\mu = 0.15$ M Tris buffer, pH 7.5, for a titration of H_2MeTri4 with [poly(dA-dT)]$_2$. The signal shifts to more positive values as the DNA-base-pair-to-porphyrin ratio q increases.

splitting (vide infra). However, exciton interactions inevitably have spectral consequences in the high loading regime (*16*), and a titration carried out at $\mu = 0.15$ M is illustrative of the effects. The absorption maximum of H_2MeTri4 shifts monotonically toward longer wavelength with the addition of [poly(dA-dT)]$_2$, but the hypochromic response maximizes in the vicinity of a base-pair-to-porphyrin ratio (q) of 6−10 before decreasing slightly to the limiting value of 18% at higher q values. At the same time, Figure 2 shows that the crossover wavelength in the induced CD spectrum shifts from 430 to 440 nm, and the positive branch becomes dominant.

Interactions with Hairpin Hosts. Previous work suggests that porphyrins bind preferentially in the stem domain of DNA hairpin, or stem−loop, structures (*35*). For all systems investigated here (Scheme 2), loop variations have a modest impact on the binding of H_2MeTri4. In each case, the Soret band of the complex shifts slightly toward longer wavelengths when 5′-gaaa-3′ replaces 5′-tttt-3′ as the loop domain. The most significant spectral change is apparent in Figure 3, which shows that the induced CD signal becomes essentially monosignate when {CA(ga$_3$)} replaces {CA(t$_4$)} as host.

Viscometry Changes. Viscometric studies involving sonicated solutions of ST DNA show that the specific viscosity (η) of the DNA polymer *increases* relative to the control upon addition of either of the triply charged porphyins (Figure 4). With the uptake of H_2Tri4, the specific viscosity increases by ca. 100% before leveling off; in contrast, the net increase is about 75% in the case of the bulkier H_2MeTri4 system.

Binding Studies of Cu(MeTri4). In a titration involving Cu(MeTri4) and [poly(dA-dT)]$_2$, the trends are qualitatively similar to those observed previously with H_2MeTri4 (see, for example, Figure 2). The absorption maximum shifts toward longer wavelength (from 422 to 432 nm), but the shift is complete by $q = 4$. However, the percentage change in absorbance ranges from +26% to −16% relative to control as q ranges from 4 to 40 during the titration. In other words, the addition of excess [poly(dA-dT)]$_2$ induces a *hyperchromic* response. Apparent hyperchromism showed up in a previous titration involving Cu(tMe$_2$D4), but the effect was due to anomalously low absorbance by the control (*16*). With Cu(tMe$_2$D4) the artifact was evident from the fact that the addition of methanol led to the dispersion of aggregates and

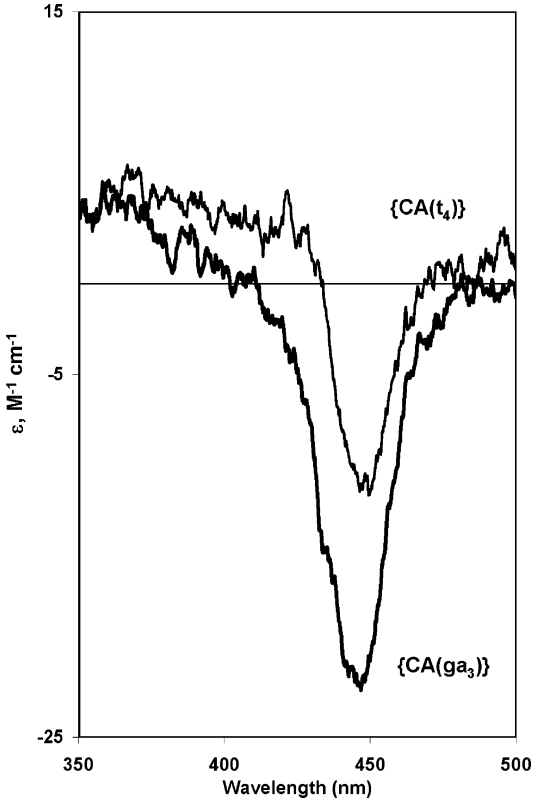

FIGURE 3: CD spectra for the complex formed by H_2MeTri4 in the presence of an excess of the DNA hairpin {CA(t$_4$)} (thin trace) versus {CA(ga$_3$)} (thick trace) in $\mu = 0.05$ M Tris buffer, pH 7.5.

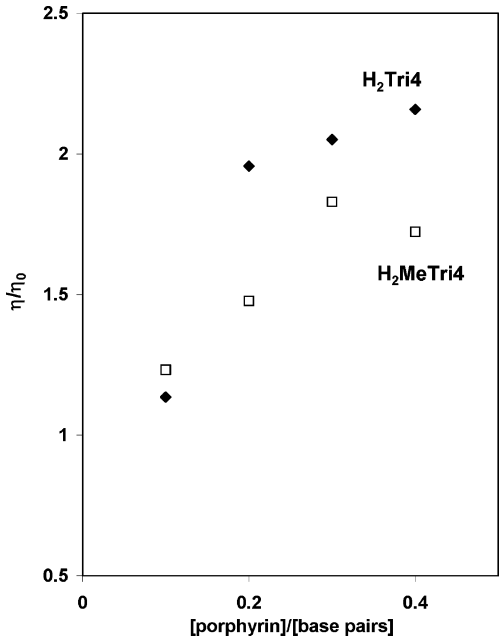

FIGURE 4: Plot of the effect the addition of H_2Tri4 (◆) or H_2-MeTri4 (□) on the specific viscosity of ST DNA in $\mu = 0.15$ M Tris buffer, pH 7.5 at 28 °C. The ordinate shows the change in viscosity relative to η_0, the viscosity in the absence of porphyrin.

enhanced absorbance in the absence of DNA. However, methanol has no significant effect on the absorbance of the more highly charged Cu(MeTri4) system, so the hyperchromism must be a consequence of complex formation with [poly(dA-dT)]$_2$. Emission studies show that free Cu(MeTri4) does not give a signal in solution, but a weak signal grows in at around 805 nm when [poly(dA-dT)]$_2$ is present.

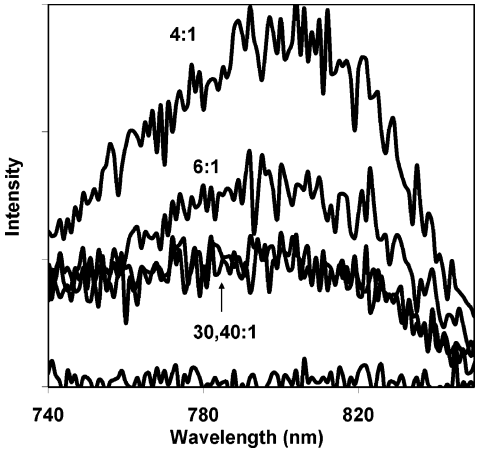

FIGURE 5: Emission from Cu(MeTri4) bound to $[poly(dA\text{-}dT)]_2$ in $\mu = 0.05$ M Tris buffer, pH 7.5. The signal intensity *decreases* as the DNA-base-pair-to-porphyrin ratio q increases.

Interestingly, the signal intensity from the bound form maximizes at $q = 4$ and then falls off before reaching a plateau that corresponds to formation of the limiting complex (Figure 5). Throughout the titration, the maximum in the emission excitation spectrum remains at around 435 nm.

DISCUSSION

Intercalation of H_2Tri4. The results in Table 1 reveal that the trisubstituted porphyrin H_2Tri4 intercalates into DNA regardless of the base composition. Due to intimate contact established with the π clouds of DNA bases, the spectral consequences of intercalative binding are quite distinctive. The signatures include a significant bathochromic shift ($\Delta\lambda \geq 15$ nm), pronounced hypochromism ($H \geq 30\%$), and a negative induced CD signal in the Soret region (*9*−*11*). Another common consequence of intercalative binding is a marked increase in the specific viscosity of ST DNA, as is evident in Figure 4. The viscosity increase occurs because intercalation of the ligand enhances both the length and rigidity of the rodlike host (*16*, *38*). In contrast, the specific viscosity may even decrease if the porphyrin binds externally to the DNA, as shown in studies involving the uptake of Zn(T4) and Zn(tMe_2D4) (*14*, *39*). Although the disubstituted porphyrins H_2D3 and H_2D4 also bind to DNA strictly by intercalation (*14*, *20*), the results obtained with H_2Tri4 are even more decisive. They demonstrate that the base dependence of the DNA binding disappears when H_2T4 has one less pyridiniumyl substituent.

Complexes Formed by H_2MeTri4 and Its Copper(II) Derivative. The tetrasubstituted H_2MeTri4 porphyrin is of interest because of its intermediate steric requirements vis à vis H_2T4 and H_2Tri4. Since H_2T4 intercalates into $[poly(dG\text{-}dC)]_2$, one would expect the same from H_2MeTri4. Confirmation of this mode of binding comes from the $\Delta\lambda$, H, and $\Delta\epsilon$ values recorded in Table 1. When $[poly(dA\text{-}dT)]_2$ acts as host, however, the induced CD signal is bisignate and indicative of the coexistence of intercalated and externally bound forms of H_2MeTri4. In principle, excitonic coupling between neighboring chromophores could also induce a bisignate CD response, as is the case when Zn(tMe_2D4) binds to $[poly(dG\text{-}dC)]_2$ (*16*). However, the Coulombic repulsions between tripositive ligands should discourage cooperative uptake and near-neighbor binding of H_2MeTri4 ligands. In keeping with that expectation, the induced CD spectrum is independent of ionic strength over the interval interval of 0.05−0.15 M. If the CD response suggests external binding is a more favorable binding motif when $[poly(dA\text{-}dT)]_2$ takes up H_2MeTri4, intercalation appears to be the preferred motif with ST DNA. Across the board, the spectral consequences of complex formation are similar, if not quite as pronounced, as those that occur with the binding of H_2Tri4. This outcome is plausible because ST DNA contains 41% G≡C base pairs and almost certainly includes extended runs of G≡C base pairs (*40*). However, Figure 4 reveals that the uptake of H_2MeTri4 induces a smaller increase in the standard reduced viscosity ratio than H_2Tri4. The differential makes sense if H_2MeTri4 also exhibits a measure of external binding within A=T-rich domains of ST DNA. The results obtained with Cu(MeTri4) are also consistent with two modes of complex formation in A=T-rich domains (vide infra). Note that a previous comparison of the absorption and emission excitation spectra of the bulkier Cu(T4) system has revealed that it, too, utilizes both binding motifs with ST DNA (*41*).

(A) Effect of the Hairpin Loop. DNA hairpins are potentially useful for studying mixed binding motifs because the composition of a hairpin is variable and the scaffold tends to be less rigid than a double-stranded DNA polymer with a like composition. Bejune and McMillin (*42*) compared the binding of Zn(D4), the zinc(II) derivative of 5,15-di(*N*-methylpyridinium-4-yl)porphyrin, with the two hairpin-forming oligos $\{TT(t_4)\}$ = 5′-GATTACttttGTAATC-3′ and $\{TT(ga_3)\}$ = 5′-GATTACgaaaGTAATC-3′. A 5′-gaaa-3′ loop enhances rigidity (*43*), and Bejune and McMillin (*42*) showed that Zn(D4) bound externally to the structure with the $\{TT(t_4)\}$ hairpin but that it preferentially intercalated into the more rigid $\{TT(ga_3)\}$ hairpin (*42*). For the same two hosts, however, complexes of H_2MeTri4 exhibit positive CD signals, consistent with purely external binding. Interest therefore shifted to the $\{CA(t_4)\}$ = 5′-GACAACttttGTTGTC-3′ and $\{CA(ga_3)\}$ = 5′-GACAACgaaaGTTGTC-3′ hairpins, because increasing the number of G≡C base pairs in the stem region tends to promote intercalation of bulky ligands like H_2T4 (*21*, *35*, *44*). As illustrated in Figure 3, the induced CD signal is largely negative when H_2MeTri4 interacts with $\{CA(t_4)\}$, so intercalation is evidently the preferred binding motif. The picture is not that simple, though, because the extremum in the CD signal occurs at a longer wavelength than the absorbance maximum. On the other hand, the extrema come into closer agreement when the more rigid hairpin, $\{CA(ga_3)\}$, serves as the host, and the crossover in the CD spectrum shifts toward shorter wavelength as well. The likely interpretation is that H_2MeTri4 binds to $\{CA(ga_3)\}$ virtually exclusively by intercalation but that there is a component of external binding to the low-melting $\{CA(t_4)\}$ host.

(B) Insights Obtained with Cu(MeTri4). Results show that there are also two types of binding when Cu(MeTri4) interacts with $[poly(dA\text{-}dT)]_2$. Particularly useful information comes from luminescence results, which show that Cu(MeTri4) intercalates into the host but not as the sole binding motif. The luminescence method is useful because a photoexcited copper(II) porphyrin is susceptible to a unique quenching mechanism, *if* it is free in solution or externally bound to DNA (*10*, *15*, *16*, *35*, *41*). However, intercalated

forms are emissive because quenching depends upon expansion of the coordination number, and internalization of the porphyrin blocks access to axial coordination sites of the metal center (*10*, *15*, *41*). In fact, intercalation is the only known mode of DNA binding that supports emission from a copper(II) porphyrin; even externally bound aggregates appear to be nonemissive (*16*). The emission results in Figure 5 therefore establish that some fraction of the Cu(MeTri4) binds to $[poly(dA\text{-}dT)]_2$ by intercalation. Intercalation is not the only mode of binding, though, because the signal is quite weak. That result, along with the observed hyperchromism, reveals that external binding is the dominant motif when Cu(MeTri4) interacts with $[poly(dA\text{-}dT)]_2$.

The intensity variation that occurs in Figure 5 is striking because the emission intensity maximizes at intermediate loading. One possible explanation is that a higher proportion of Cu(MeTri4) intercalates when there is less DNA present in solution. This outcome is plausible if intercalated Cu(MeTri4) has a smaller footprint than the externally bound form because simple space considerations would favor intercalative binding when $[poly(dA\text{-}dT)]_2$ is the limiting reagent. Another explanation could be that the emission maximizes because heavy loading enhances the rigidity of the host−guest system and moderates the rate of nonradiative decay. Either way, the distance between chromophores is smaller in the intermediate loading regime, and one should expect exciton interactions to become evident in the CD spectrum (*16*). In fact, the amplitude of the negative branch of the CD signal maximizes at intermediate loading of Cu(MeTri4), at a base-pair-to-porphyrin ratio of $q \approx 4$. Upon addition of more DNA, the intensity of the negative component decreases and then plateaus, similar to the results in Figure 2 for H_2MeTri4.

Orientation of the Intercalator. Between any two base pairs, intercalation of H_2Tri4 or H_2MeTri4 can occur in two ways. This conclusion follows from X-ray crystallographic (*18*) and NMR studies (*19*), which have shown that intercalation of H_2T4 involves inserting two meso substituents into each groove of the DNA host. In the case of H_2Tri4, therefore, the porphyrin can extend either one *N*-methylpyridinium-4-yl group and the C20 hydrogen or two *N*-methylpyridinium-4-yl groups into the minor groove. The latter isomer would of course suffer the same steric strain that destabilizes the intercalated form of H_2T4. On the other hand, electrostatic forces favor that orientation because the electrostatic potential of $[poly(dA\text{-}dT)]_2$ is thought to be more negative in the minor groove (*45*). (An underlying assumption is that the normal complement of sodium ions is in place about the canonical sugar−phosphate backbone structure.) Although direct evidence is lacking, it seems safe to conclude that the porphyrins avoid steric problems and extend only one of their bulky *N*-methylpyridinium-4-yl groups into the minor groove. Otherwise it is hard to explain why H_2MeTri4 preferentially binds externally to $[poly(dA\text{-}dT)]_2$, when H_2Tri4 binds by intercalation. A methyl group would hardly have that kind of impact if it were relegated to the comparatively spacious major groove.

Base Specificity of Binding. There is as yet no consensus about why H_2T4 and its various metalated forms bind externally to A=T-rich sequences of DNA. Part of the difficulty is the lack of unambiguous structural information, even as regards the groove preference. In a published crystal structure, a Ni(T4) ligand caps the end of one duplex and interacts edge-on with the minor groove of another (*46*). In contrast, published NMR data are more consistent with a major-groove approach when H_2T4 interacts with an 8-mer duplex (*24*). One view is that electrostatic effects and/or the groove structure may predispose sequences that are rich in A=T base pairs toward the external binding of cationic porphyrins (*22*, *23*). However, Wilson and co-workers (*47*) have pointed out that high-affinity groove binders tend to have a crescent shape, positive charge, inward-facing hydrogen-bonding groups, and an extended unfused heterocyclic structure. That is not exactly the prescription of a system like H_2T4. Moreover, if external binding depends upon an edge-on approach to the minor groove of the DNA host (*12*), one would expect the C5 methyl substituent of H_2MeTri4 to pose steric problems and inhibit uptake, yet H_2MeTri4 is more prone to external binding than H_2Tri4. An alternative model focuses on the destabilizing forces associated with uptake of the porphyrin (*14*, *15*). One of the early suggestions along these lines was that H_2T4 binds externally to A=T-rich sequences because steric clashes with thymine methyl groups interfere with the intercalation of H_2T4 (*48*). Subsequent base-replacement studies cast doubt on the hypothesis, however (*49*). It now seems clear that destabilization of the intercalated form is due to *steric problems in the minor groove*, which is relatively narrow, especially in A=T-rich duplexes. An A=T-rich sequence is sufficiently flexible that a structural change is possible, of course, but therein lies the opportunity for local melting and concomitant formation of a pocket suitable for high-affinity external binding as well (*9*, *14*−*16*). Contrariwise, the presence of G≡C base pairs poses a considerable barrier to the same type of reorganization due to the extra hydrogen bond between base pairs that reinforces the canonical B-form DNA structure. In this view the *rigidity of a G≡C-rich* sequence explains why external binding of the axially ligated porphyrin Zn(T4) is a comparatively low-affinity process with $[poly(dG\text{-}dC)]_2$ (*15*, *50*). In closing, it is worth emphasizing that attractive interactions influence the binding motif as well. As a reviewer has noted, intercalators often prefer G≡C-rich sequences.

CONCLUSIONS

The results described herein expose the intertwined roles that electrostatic and steric forces play in determining whether or not a cationic porphyrin intercalates into B-form DNA. The key observation is that trisubstituted H_2Tri4 binds as an intercalator irrespective of the base composition of the host. However, H_2Tri4 proves to be a limiting case. Introducing even a methyl group at the other methine carbon position increases the steric demand enough that external binding becomes the preferred binding motif for $[poly(dA\text{-}dT)]_2$. The balance between electrostatic and steric forces involved in binding porphyrins can be exquisite. Methyl and *N*-methylpyridinium-4-yl substituents can coexist in the minor groove of $[poly(dA\text{-}dT)]_2$ because the dicationic H_2tMe_2D4 system binds by intercalation, though not without some steric strain (*16*). On the other hand, Wu and co-workers (*51*) have reported that the slightly larger ligand, 5,15-diethyl-10,20-di(*N*-methylpyridinium-4-yl)porphyrin, binds externally to calf thymus DNA as well as by intercalation. Despite the fact that other factors may be at work, antagonistic factors clearly play important roles in determining how the base

content shapes the binding motif, much like poisoning effects give rise to substrate specificity in a catalytic process. Steric forces destabilize the intercalated form of a bulky porphyrin, whereas external binding exacts a toll on the host structure. Hence, trisubstituted H_2Tri4 binds strictly by intercalation, despite a nonideal charge alignment with the DNA backbone.

REFERENCES

1. Henderson, B. W., and Dougherty, T. J. (1992) How Does Photodynamic Therapy Work, *Photochem. Photobiol. 55*, 145−157.
2. Lane, N. (2003) New light on medicine, *Sci. Am. 288* (1), 38−45.
3. Caminos, D. A., and Durantini, E. N. (2006) Photodynamic inactivation of *Escherichia coli* immobilized on agar surfaces by a tricationic porphyrin, *Bioorg. Med. Chem. 14*, 4253−4259.
4. Snyder, J. W., Lambert, J. D. C., and Ogilby, P. R. (2006) 5,10,-15,20-Tetrakis(*N*-methyl-4-pyridyl)-21*H*,23*H*-porphine (TMPyP) as a sensitizer for singlet oxygen imaging in cells: Characterizing the irradiation-dependent behavior of TMPyP in a single cell, *Photochem. Photobiol. 82*, 177−184.
5. Davis, J. T. (2004) G-quartets 40 years later: From 5′-GMP to molecular biology and supramolecular chemistry, *Angew. Chem., Int. Ed. 43*, 668−698.
6. Shi, D. F., Wheelhouse, R. T., Sun, D. Y., and Hurley, L. H. (2001) Quadruplex-interactive agents as telomerase inhibitors: Synthesis of porphyrins and structure−activity relationship for the inhibition of telomerase, *J. Med. Chem. 44*, 4509−4523.
7. Goncalves, D. P. N., Ladame, S., Balasubramanian, S., and Sanders, J. K. M. (2006) Synthesis and G-quadruplex binding studies of new 4-*N*-methylpyridinium porphyrins, *Org. Biomol. Chem. 4*, 3337−3342.
8. Wei, C. Y., Jia, G. Q., Yuan, J. L., Feng, Z. C., and Li, C. (2006) A spectroscopic study on the interactions of porphyrin with G-quadruplex DNAs, *Biochemistry 45*, 6681−6691.
9. Pasternack, R. F., and Gibbs, E. J. (1996) Porphyrin and metalloporphyrin interactions with nucleic acids, *Met. Ions Biol. Syst. 33*, 367−397.
10. McMillin, D. R., and McNett, K. M. (1998) Photoprocesses of copper complexes that bind to DNA, *Chem. Rev. 98*, 1201−1219.
11. Marzilli, L. G. (1990) Medical Aspects of DNA−Porphyrin Interactions, *New J. Chem. 14*, 409−420.
12. Pitié, M., Boldron, C., and Pratviel, G. (2006) DNA oxidation by copper and manganese complexes, *Adv. Inorg. Chem. 58*, 77−130.
13. Pasternack, R. F., Gibbs, E. J., and Villafranca, J. J. (1983) Interactions of Porphyrins with Nucleic Acids, *Biochemistry 22*, 2406−2414.
14. Bejune, S. A., Shelton, A. H., and McMillin, D. R. (2003) New Dicationic Porphyrin Ligands Suited for Intercalation into B-Form DNA, *Inorg. Chem. 42*, 8465−8475.
15. McMillin, D. R., Shelton, A. H., Bejune, S. A., Fanwick, P. E., and Wall, R. K. (2005) Understanding Binding Interactions of Cationic Porphyrins with B-form DNA, *Coord. Chem. Rev. 249*, 1451−1459.
16. Shelton, A. H., Rodger, A., and McMillin, D. R. (2007) DNA Binding Studies of a New Dicationic Porphyrin. Insights into Interligand Interactions, *Biochemistry 46*, 9143−9154.
17. Sari, M. A., Battioni, J. P., Dupre, D., Mansuy, D., and Lepecq, J. B. (1990) Interaction of Cationic Porphyrins with DNA: Importance of the Number and Position of the Charges and Minimum Structural Requirements for Intercalation, *Biochemistry 29*, 4205−4215.
18. Lipscomb, L. A., Zhou, F. X., Presnell, S. R., Woo, R. J., Peek, M. E., Plaskon, R. R., and Williams, L. D. (1996) Structure of a DNA−Porphyrin complex, *Biochemistry 35*, 2818−2823.
19. Guliaev, A. B., and Leontis, N. B. (1999) Cationic 5,10,15,20-tetrakis(*N*-methylpyridinium-4-yl)porphyrin fully intercalates at 5′-CG-3′ steps of duplex DNA in solution, *Biochemistry 38*, 15425−15437.
20. Wall, R. K., Shelton, A. H., Bonaccorsi, L. C., Bejune, S. A., Dube, D., and McMillin, D. R. (2001) H_2D3: A cationic porphyrin designed to intercalate into B-form DNA (H_2D3 = *trans*-di(*N*-methylpyridium-3-yl)porphyrin), *J. Am. Chem. Soc. 123*, 11480−11481.
21. Tears, D. K. C., and McMillin, D. R. (1998) Duplex hydrogen banding promotes intercalation of Cu(T4) in DNA hairpins (Cu(T4) = *meso*-tetrakis(4-(*N*-methylpyridyl))porphyrincopper(II)), *Chem. Commun. (Cambridge, U.K.)*, 2517−2518.
22. Marzilli, L. G., Petho, G., Lin, M. F., Kim, M. S., and Dixon, D. W. (1992) Tentacle Porphyrins: DNA Interactions, *J. Am. Chem. Soc. 114*, 7575−7577.
23. Mukundan, N. E., Petho, G., Dixon, D. W., and Marzilli, L. G. (1995) DNA−Tentacle Porphyrin Interactions: AT Over GC Selectivity Exhibited By An Outside Binding Self-Stacking Porphyrin. *Inorg. Chem. 34*, *3677−3687*.
24. Ohyama, T., Mita, H., and Yamamoto, Y. (2005) Binding of 5,-10,15,20-tetrakis(*N*-methylpyridinium-4-yl)-21*H*,23*H*-porphyrin to an AT-rich region of a duplex DNA. *Biophys. Chem. 113*, 53−59.
25. Lindsey, J. S. (1999) Synthesis of meso-Substituted Porphyrins, in *The Porphyrin Handbook* (Kadish, K. M., Smith, K. M., and Guilard, R., Eds.) pp 45−118, Academic Press, New York.
26. Vicente, M. G. H., and Smith, K. M. (2000) Porphyrins and derivatives: Synthetic strategies and reactivity profiles. *Curr. Org. Chem. 4*, 139−174.
27. Gryko, D., and Lindsey, J. S. (2000) Rational synthesis of meso-substituted porphyrins bearing one nitrogen heterocyclic group, *J. Org. Chem. 65*, 2249−2252.
28. Batinic-Haberle, I., Spasojevic, I., Hambright, P., Benov, L., Crumbliss, A. L., and Fridovich, I. (1999) Relationship among redox potentials, proton dissociation constants of pyrrolic nitrogens, and in vivo and in vitro superoxide dismutating activities of manganese(III) and iron(III) water-soluble porphyrins, *Inorg. Chem. 38*, 4011−4022.
29. Ryppa, C., Senge, M. O., Hatscher, S. S., Kleinpeter, E., Wacker, P., Schilde, U., and Wiehe, A. (2005) Synthesis of mono- and disubstituted porphyrins: A- and 5,10-A_2-type systems, *Chem.—Eur. J. 11*, 3427−3442.
30. Sambrook, J., Fritsch, J., and Maniatis, T. (1989) *Molecular Cloning: A Laboratory Manual*, 2nd ed., Cold Spring Harbor Laboratory Press, Cold Spring Harbor, NY.
31. Pasternack, R. F., Francesconi, L., Raft, D., and Spiro, E. (1973) Aggregation of Nickel(II), Copper(II), and Zinc(II) Derivatives of Water-Soluble Porphyrins, *Inorg. Chem. 12*, *2606−2611*.
32. Inman, R. B., and Baldwin, R. L. (1962) Helix−Random Coil Transitions in Synthetic DNAs of Alternating Sequence, *J. Mol. Biol. 5*, 172−184.
33. Grant, R. C., Wells, R. D., and Kodama, M. (1972) Enzymatic and Physical Studies on $(dI\text{-}dC)_n\cdot(dI\text{-}dC)_n$ and $(dG\text{-}dC)_n\cdot(dG\text{-}dC)_n$, *Biochemistry 11*, 805−815.
34. Felsenfeld, G., and Hirschman, S. Z. (1965) A Neighbor-Interaction Analysis of the Hypochromism and Spectra of DNA, *J. Mol. Biol. 13*, 407−427.
35. Lugo-Ponce, P., and McMillin, D. R. (2000) DNA-binding studies of Cu(T4), a bulky cationic porphyrin, *Coord. Chem. Rev. 208*, 169−191.
36. Cantor, C. R., Warshaw, M. M., and Shapiro, H. (1970) Oligonucleotide Interactions. 3. Circular Dichroism Studies of Conformation of Deoxyoligonucleotides, *Biopolymers 9*, 1059−1077.
37. Satyanarayana, S., Dabrowiak, J. C., and Chaires, J. B. (1992) Neither Δ-Tris(Phenanthroline)Ruthenium(II) nor Δ-Tris(Phenanthroline)Ruthenium(II) Binds to DNA by Classical Intercalation, *Biochemistry 31*, 9319−9324.
38. Banville, D. L., Marzilli, L. G., Strickland, J. A., and Wilson, W. D. (1986) Comparison of the Effects of Cationic Porphyrins on DNA Properties: Influence of GC Content of Native and Synthetic Polymers, *Biopolymers 25*, 1837−1858.
39. Pasternack, R. F., Gibbs, E. J., and Villafranca, J. J. (1983) Interactions of Porphyrins with Nucleic Acids, *Biochemistry 22*, 2406−2414.
40. Felix, K., Jilke, I., and Zahn, R. K. (1956) Die Desoxyribonucleinsaure Einiger Fischspermien, *Hoppe-Seyler's Z. Physiol. Chem. 303*, 140−152.
41. Hudson, B. P., Sou, J., Berger, D. J., and McMillin, D. R. (1992) Luminescence Studies of the Intercalation of Cu(TMPyP4) into DNA, *J. Am. Chem. Soc. 114*, 8997−9002.
42. Bejune, S. A., and McMillin, D. R. (2004) The influence of the loop sequence in binding studies involving cationic porphyrins and DNA hairpins, *Chem. Commun. (Cambridge, U.K.)* 1320−1321.
43. Nakano, M., Moody, E. M., Liang, J., and Bevilacqua, P. C. (2002) Selection for thermodynamically stable DNA tetraloops using temperature gradient gel electrophoresis reveals four motifs:

d(cGNNAg), d(cGNABg), d(cCNNGg), and d(gCNNGc), *Biochemistry 41*, 14281−14292.

44. Eggleston, M. K., Crites, D. K., and McMillin, D. R. (1998) Studies of the base-dependent binding of Cu(T4) to DNA hairpins (H_2T4 = *meso*-Tetrakis(4-(*N*-methylpyridiumyl))porphyrin), *J. Phys. Chem. A 102*, 5506−5511.
45. Lavery, R., and Pullman, B. (1985) The Dependence of the Surface Electrostatic Potential of B-DNA on Environmental Factors, *J. Biomol. Struct. Dyn. 2*, 1021−1032.
46. Bennett, M., Krah, A., Wien, F., Garman, E., McKenna, R., Sanderson, M., and Neidle, S. (2000) A DNA−porphyrin minor-groove complex at atomic resolution: The structural consequences of porphyrin ruffling, *Proc. Natl. Acad. Sci. U.S.A. 97*, 9476−9481.
47. Tanious, F. A., Laine, W., Peixoto, P., Bailly, C., Goodwin, K. D., Lewis, M. A., Long, E. C., Georgiadis, M. M., Tidwell, R. R., and Wilson, W. D. (2007) Unusually strong binding to the DNA minor groove by a highly twisted benzimidazole diphenylether: Induced fit and bound water, *Biochemistry 46*, 6944−6956.
48. Ford, K., Fox, K. R., Neidle, S., and Waring, M. J. (1987) DNA-Sequence Preferences for an Intercalating Porphyrin Compound Revealed by Footprinting, *Nucleic Acids Res. 15*, 2221−2234.
49. Thomas, K. E., and McMillin, D. R. (2001) Competitive binding studies of H_2T4 with DNA hairpins (H_2T4 = *meso*-tetrakis(4-(*N*-methylpyridiniumyl))porphyrin), *J. Phys. Chem. B 105*, 12628−12633.
50. Strickland, J. A., Marzilli, L. G., Gay, K. M., and Wilson, W. D. (1988) Porphyrin and Metalloporphyrin Binding to DNA Polymers: Rate and Equilibrium Binding Studies, *Biochemistry 27*, 8870−8878.
51. Wu, S., Li, Z., Ren, L. G., Chen, B., Liang, F., Zhou, X., Jia, T., and Cao, X. P. (2006) Dicationic pyridium porphyrins appending different peripheral substituents: Synthesis and studies for their interactions with DNA, *Bioorg. Med. Chem. 14*, 2956−2965.

BI7018755